

SPACE RADIATION PECULIARITIES IN THE EXTRA VEHICULAR ENVIRONMENT OF THE INTERNATIONAL SPACE STATION (ISS)

***Tsvetan Dachev, Nikolay Bankov, Borislav Tomov,
Yury Matviichuk, Plamen Dimitrov***

*Space Research and Technology Institute – Bulgarian Academy of Sciences
e-mail: tdachev@bas.bg*

Abstract

The space weather and the connected with it ionizing radiation were recognized as a one of the main health concern to the International Space Station (ISS) crew. Estimation the effects of radiation on humans in ISS requires at first order accurate knowledge of the accumulated by them absorbed dose rates, which depend of the global space radiation distribution and the local variations generated by the 3D surrounding shielding distribution. The R3DE (Radiation Risks Radiometer-Dosimeter (R3D) for the EXPOSE-E platform on the European Technological Exposure Facility (EuTEF) worked successfully outside of the European Columbus module between February 2008 and September 2009. Very similar instrument named R3DR for the EXPOSE-R platform worked outside Russian Zvezda module of ISS between March 2009 and August 2010. Both are Liulin type, Bulgarian build miniature spectrometers-dosimeters. They accumulated about 5 million measurements of the flux and absorbed dose rate with 10 seconds resolution behind less than 0.41 g cm^{-2} shielding, which is very similar to the Russian and American space suits [1-3] average shielding. That is why all obtained data can be interpreted as possible doses during Extra Vehicular Activities (EVA) of the cosmonauts and astronauts. The paper first analyses the obtained long-term results in the different radiation environments of: Galactic Cosmic Rays (GCR), inner radiation belt trapped protons in the region of the South Atlantic Anomaly (SAA) and outer radiation belt (ORB) relativistic electrons. The large data base was used for development of an empirical model for calculation of the absorbed dose rates in the extra vehicular environment of ISS at 359 km altitude. The model approximate the averaged in a grid empirical dose rate values to predict the values at required from the user geographical point, station orbit or area in geographic coordinate system. Further in the paper it is presented an intercomparison between predicted by the model dose rate values and data collected by the R3DE/R instruments and NASA Tissue Equivalent Proportional Counter (TEPC) during real cosmonauts and astronauts EVA in

the 2008-2010 time interval including large relativistic electrons doses during the magnetosphere enhancement in April 2010. The model was also used to be predicted the accumulated along the orbit of ISS galactic cosmic rays and inner radiation belt dose for 1 orbit (1.5 hours) and 4 consequent orbits (6 hours), which is the usual EVA continuation in dependence by the longitude of the ascending node of ISS. These predictions of the model could be used by space agencies medical and other not specialized in the radiobiology support staff for first approach in the ISS EVA time and space planning.

1. Introduction

The radiation field around the ISS is complex, composed by galactic cosmic rays (GCR), trapped radiation of the Earth radiation belts, solar energetic particles, albedo particles from Earth's atmosphere and secondary radiation produced in the shielding materials of the spacecraft and in biological objects.

1.1. Galactic cosmic rays

The dominant radiation component in near Earth space environment are the galactic cosmic rays (GCR) modulated by the solar activity. The GCR are charged particles that originate from sources beyond our solar system. They are thought to be accelerated at the highly energetic sources like neutron star, black holes and supernovae within our Galaxy. GCR are the most penetrating of the major types of ionizing radiation. The distribution of GCR is believed to be isotropic throughout interstellar space. The energies of GCR particles range from several tens up to 10^{12} MeV nucleon⁻¹. The GCR spectrum consists of 98% protons and heavier ions (baryon component) and 2% electrons and positrons (lepton component). The baryon component is composed of 87% protons, 12% helium ions (alpha particles) and 1% heavy ions [4]. Highly energetic particles in the heavy ion component, typically referred to as high Z and energy (HZE) particles, play a particularly important role in space dosimetry (Benton and Benton, 2001). HZE particles, especially iron, possess high-LET and are highly penetrating, giving them a large potential for radiobiological damage [5]. Up to 1 GeV, the flux and spectra of GCR particles are strongly influenced by the solar activity and hence shows modulation which is anti-correlated with solar activity.

1.2. Trapped radiation belts

Radiation belts are the regions of high concentration of the energetic electrons and protons trapped within the Earth's magnetosphere. There are

two distinct belts of toroidal shape surrounding Earth where the high energy charged particles get trapped in the Earth's magnetic field. Energetic ions and electrons within the Earth's radiation belts pose a hazard to both astronauts and spacecraft. The inner radiation belt, located between about 0.1 to 2 Earth radii, consists of both electrons with energies up to 10 MeV and protons with energies up to ~ 100 MeV. The outer radiation belt (ORB) starts from about 4 Earth radii and extends to about 9-10 Earth radii in the anti-sun direction. The outer belt mostly consists of electrons whose energy is not larger than 10 MeV. The electron flux may cause problems for components located outside a spacecraft (e.g. solar cell degradation). They do not have enough energy to penetrate a heavily shielded spacecraft such as the ISS wall, but may deliver large additional doses to astronauts during extra vehicular activity [6-8]. The main absorbed dose inside the ISS is contributed by the protons of the inner radiation belt. The South-Atlantic Anomaly (SAA) is an area where the radiation belt comes closer to the Earth surface owing to a displacement of the magnetic dipole axes from the Earth's center. The daily average SAA doses reported by Reitz et al. (2005) [9] inside of the ISS vary in the range $74\text{-}215 \mu\text{Gy d}^{-1}$ for the absorbed dose rates and in the range $130\text{-}258 \mu\text{Sv d}^{-1}$ for the averaged equivalent daily dose rates.

1.3. Solar Energetic Particles (SEP)

The SEP are mainly produced by solar flares, sudden sporadic eruptions of the chromosphere of the Sun. High fluxes of charged particles (mostly protons, some electrons and helium and heavier ions) with energies up to several GeV are emitted by processes of acceleration outside the Sun. The time profile of a typical SEP starts off with a rapid exponential increase in flux, reaching a peak in minutes to hours. The energy emitted lies between 15 and $500 \text{ MeV nucleon}^{-1}$ and the intensity can reach $10^4 \text{ cm}^{-2} \text{ s}^{-1} \text{ sr}^{-1}$. Electrons with energies of ~ 0.5 to 1 MeV arrive at Moon, usually traveling along interplanetary field lines, within tens of minutes to tens of hours. Protons with energies of 20 to 80 MeV arrive within a few to ~ 10 hours, although some high energy protons can arrive in as little as 20 minutes. SEP are relatively rare and occur most often during the solar maximum phase of the 11-year solar cycle. In the years of maximum solar activity up to 10 flares can occur, during the years of minimum solar activity only one event can be observed on average

The radiation field at a location, either outside or inside the spacecraft is affected both by the shielding and surrounding materials [10-12]. Dose characteristics in LEO depend also on many other parameters such as the solar cycle phase, spacecraft orbit parameters, helio and geophysical parameters.

Recently the radiation environment inside and outside of ISS has been studied with various arrangements of radiation detectors. The paper first analyses the obtained long-term results in the different radiation environments of: Galactic Cosmic Rays (GCR), inner radiation belt trapped protons in the region of the South Atlantic Anomaly (SAA) and outer radiation belt (ORB) relativistic electrons. The dose rates and fluxes was measured in 2008-2009 by the R3DE active dosimeter, mounted in EXPOSE-E facility outside the Columbus module of ISS and by the R3DR active dosimeter in EXPOSE-R facility outside the Russian Zvezda module of the ISS.

2. Instrumentation



Fig. 1. External view of R3DE instrument. R3DR instrument is with very similar external view

The (Radiation Risks Radiometer-Dosimeter (R3D) R3DE and R3DR instruments (Figure 1) are successors of the Liulin-E094 instrument, which was part of the experiment Dosimetric Mapping-E094 headed by Dr. G. Reitz that was placed in the US Laboratory Module of the ISS as a part of Human Research Facility of Expedition Two Mission 5A.1 in May-August, 2001 [9, 13-17].

The experiments with the R3DE/R spectrometers were performed after successful participations to ESA Announcements of Opportunities, led by German colleagues Gerda Horneck [18] and Donat-P. Häder. The spectrometers were mutually developed with the colleagues from the University in Erlangen, Germany [32, 33]. The R3DE instrument for the EXPOSE-E facility on the European Technological Exposure Facility (EuTEF) worked outside of the European Columbus module of the ISS between 20th of February 2008 and 1st of September 2009 with 10 seconds resolution behind less than 0.4 g.cm⁻² shielding.

The R3DR spectrometer was launched inside of the EXPOSE-R



Fig. 2. External view of the EXPOSE-R facility. The R3DR instrument was situated inside of the red oval. EXPOSE-E facility was with very similar external view

facility (Figure 2) to the ISS in December 2008 and was mounted at the outside platform of Russian Zvezda module of the ISS. The first data were received on March 11, 2009. Until 27th of January 2011 the instrument worked almost permanently with 10 seconds resolution.

The exact mounting locations of the both instruments are seen in Figure 3. The Figure is discussed comprehensively in the data analysis part of the paper.

R3DE/R instruments was a low mass, small dimensions automatic devices that measures solar radiation in 4 channels and ionizing radiation in 256 channels. The 4 solar UV and visible radiations photodiodes are seen in the center of the Figure 1, while the silicon detector is behind the aluminum box of the instrument; that is why is not seen in the picture. It is situated above the 4 photodiodes. They are Liulin type energy deposition

spectrometers [13] (Dachev et al., 2002). The four optical channels use 4 photodiodes with enhanced sensitivity in the following ultraviolet (UV) and visible ranges: UV-A (315-400 nm), UV-B (280-315 nm), UV-C (<280 nm) and Photosynthetic Active Radiation (PAR) (400-700 nm). They are constructed as filter dosimeters and measure the solar UV irradiance in W/m^2 . Additional measurements of the temperature of UV photodiodes are performed for more precise UV irradiance assessments. The size of the aluminum box of the R3DR instrument is 76 x 76 x 34 mm.

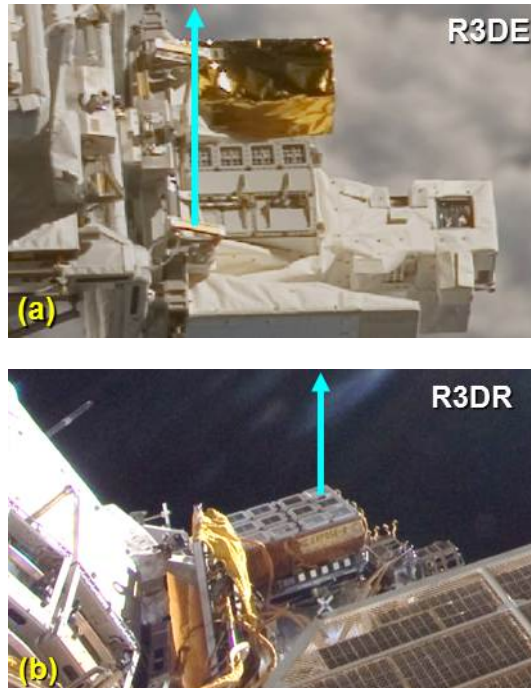


Fig. 3. Real photographs of the mounting positions of the EXPOSE-E/R facilities. The bases of the arrows show the exact places of R3DE/R instruments

The block diagram of the instruments is shown in Figure 4. Two microprocessors control the ionizing and the solar radiation circuitry, respectively, and the data are transmitted by standard serial interface of RS422 type through the EXPOSE-E/R facilities to the telemetry of Columbus module or Russian segment of the ISS. The photodiodes and the silicon detector are placed close to the preamplifiers to keep the noise level low. The signals from the solar radiation channels and the temperature

sensor are digitized by a 12 bit A/D converter. The analysis of these data is performed by the University of Erlangen, Germany (<http://www.zellbio.nat.unierlangen.de/forschung/lebert/index.shtml>).

The ionizing radiation is monitored using a semiconductor PIN diode detector (2 cm² area and 0.3 mm thick). Its signal is digitized by a 12 bit fast A/D converter after passing a charge-sensitive preamplifier. The deposited energies (doses) are determined by a pulse height analysis

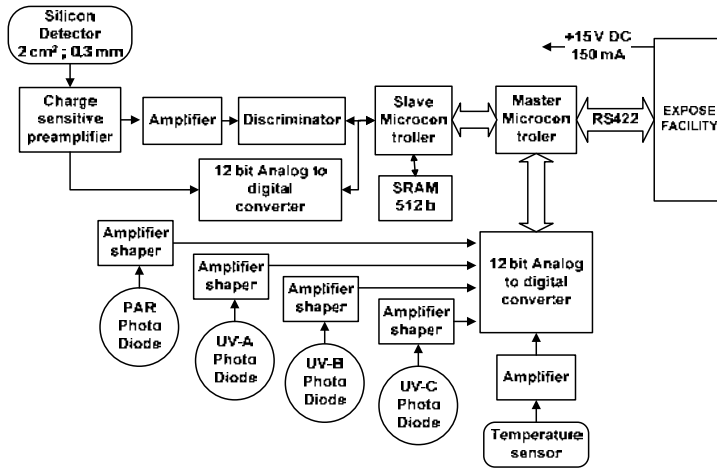


Fig. 4. Block diagram of the R3DE/R instruments

technique and then passed to a discriminator. The amplitudes of the pulses $A[V]$ are transformed into digital signals, which are sorted into 256 channels by a multi-channel analyzer. At every exposure time interval one energy deposition spectrum is collected. The energy channel number 256 accumulates all pulses with amplitudes higher than the maximal level of the spectrometer of 20.83 MeV. The methods for characterization of the type of incoming space radiation are described in (Dachev, 2009).

The “System international (SI)” determination of the dose is used, in order to calculate the doses absorbed in the silicon detector. SI determines that the dose is the energy in Joules deposited in one kilogram. The following equation is used:

$$(1) \quad D[Gy] = K \sum_{i=1}^{256} (EL_i i)[J] / MD[kg]$$

where K is a coefficient, MD - the mass of the solid state detector in [kg] and EL_i is the energy loss in Joules in channel i . The energy in MeV is proportional to the amplitude A of the pulse and the coefficient depends on the used preamplifier and sensitivity.

$$EL_i [MeV] = A[V] / 0.24[V / MeV] \cdot 0.24[V / MeV]$$

The construction of the R3DE/R boxes consists of 1.0 mm thick aluminum shielding in front of the detector. The total shielding of the detector is formed by additional internal constructive shielding of 0.1 mm copper and 0.2 mm plastic material. The total external and internal shielding before the detector of R3DR device is 0.41 g cm^{-2} . The calculated stopping energy of normally incident particles to the detector is 0.78 MeV for electrons and 15.8 MeV for protons [19]. This means that only protons and electrons with energies higher than the above mentioned could reach the detector.

3. Data analysis

3.1. Global distribution

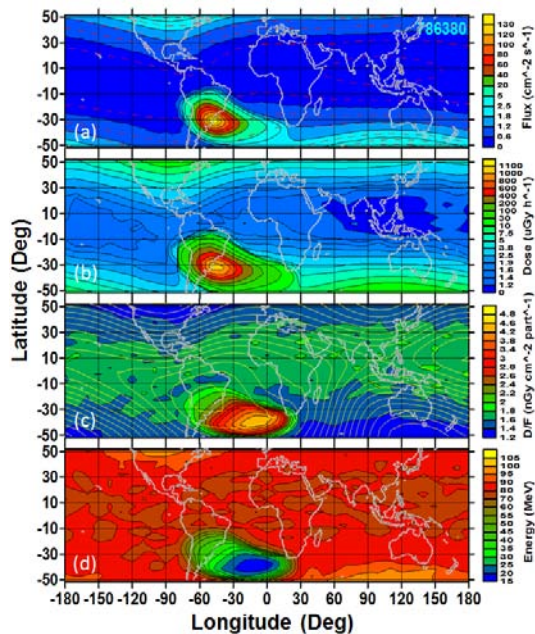


Fig. 5. Global distribution of the R3DE dose rate, flux, D/F ratio and incident energy data in the period 21 October 2008-24 February 2009

Figure 5 presents the global view on the R3DE dose rate, flux and energy data for the time period between 21/10/2008 and 24/02/2009. The ISS altitude for this period varies between 364 and 375 km. The first 2 panels contain 786380 measurements of the flux in the upper panel and of the absorbed dose rate in the panel below. On the Figure 5a except the global map of the flux the isolines of the L value [20, 21] at the altitude of the ISS are also presented with red dashed lines. It is seen that the lines of equal flux in the north and south high latitude regions follow very well the L-shell isolines as expected. The place and area of the South Atlantic Magnetic Anomaly (SAA) is well seen by the last close isoline of 0.26 Gauss on Figure 5c. Because of relative low magnetic field strength in the SAA the protons in the inner radiation belt penetrated deeper in the upper atmosphere and reach the altitude of the station forming large maximums of the flux and dose respectively. Both the flux and dose rate maximums was displaced from the magnetic field minimum in South-East direction, while the dose rate maximum goes even further to the same direction.

On the Figure 5c the global distribution of the dose to flux ratio (D/F) in $\text{nGy cm}^{-2} \text{ particle}^{-1}$ is presented. 247277 measurement points was used. D/F ratios larger than $1 \text{ nGy cm}^{-2} \text{ particle}^{-1}$ was selected and plotted. It is seen that the ratio form a maximum with D/F value greater than $4 \text{ nGy cm}^{-2} \text{ particle}^{-1}$ in the South-East edge of the anomaly. The global distribution of the calculated from the D/F ratio incident energy of the arriving to the detector inner radiation belt protons [22, 30] (Heffner, 1971; Dachev, 2009) was presented at the Figure 4d and as expected form a minimum at the places of the dose to flux ratio maximum in the Figure 4c. The center of the 15-20 MeV protons maximum is with coordinates 15°W , 38°S . This result is controversial than the AP-8 MIN [23, 24] predictions, which show the place of the maximum almost at same latitude but at about 38° west longitude.

The GCR dose and flux global distribution is presented in the Figures 5a and 5b with all areas outside the SAA region. It forms wide minimum close to the geomagnetic equator and rise toward the magnetic poles in both hemispheres (For more information please look Fig.6). For the regions outside the SAA the calculated values for the dose to flux ratio and for the incident energies presented in the Figures 5c and 5d are not valid because of the small statistics in the spectra.

3.2. R3DE/R data comparison

Figure 6 presents in 2 panels the dose rate (black (dark blue) points) and flux data (gray (sky blue) points) obtained in the 10-20 April 2009 time

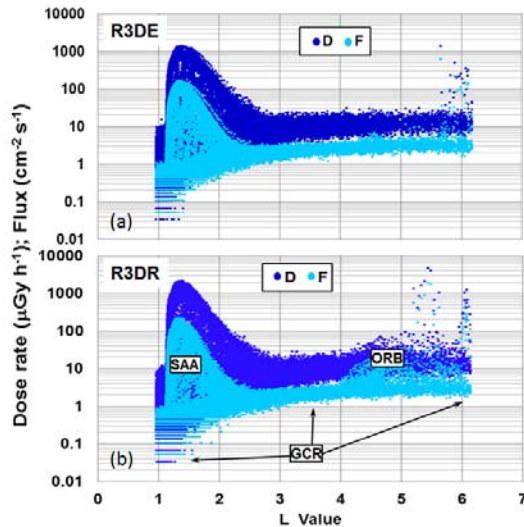


Fig. 6. Comparison of the dose rate and flux data measured with 10 s resolution by the R3DE/R instruments in the period 10-20 April 2009

interval as measured with 10 s resolution by the R3DE/R instruments. The bottom panel (Figure 6b) contains data from the R3DR instrument, while the top panel (Figure 6a) contain data from the R3DE instrument.

Three different radiation sources are easily distinguished visually from the data presented in both panels. The major amount of measurements with more than 7000 points per day is concentrated in the zone of GCR, which is seen as area with many points in the lower part of the panels in L-values range between 0.9 and 6.2. The covered dose rate range is between 0.03 and 15-20 $\mu\text{Gy h}^{-1}$. The lowest rates are close to the magnetic equator ($L < 1.5$), while the highest are at high latitudes ($L > 4$) equatorwards from both magnetic poles.

The maximum of the inner radiation belt protons observed in the region of the SAA is seen in the left side of the panels with dose rates between 10 and 1250 $\mu\text{Gy h}^{-1}$ from R3DR instrument (Figure 6b), while the

maximum from R3DE instrument is smaller and reach $1100 \mu\text{Gy h}^{-1}$ (Figure 6a).

The reason of R3DR SAA dose rates being higher than the R3DE dose rates is seen in Figure 3. The 2 photographs on Figure 3 presented the surrounding of the R3DE and R3DR instruments on ISS. As mentioned before, R3DE was located at the top of the EuTEF platform outside the European Columbus module.

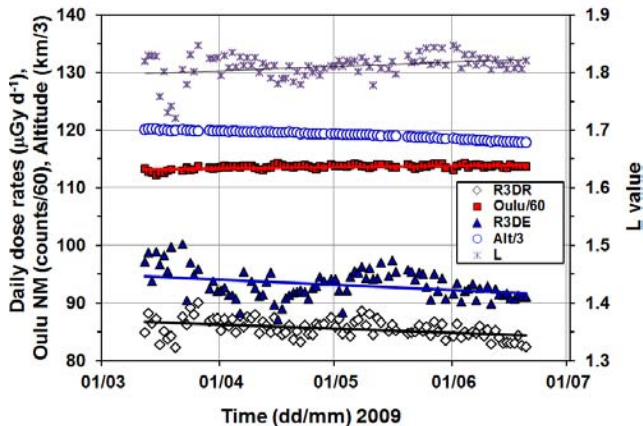


Fig. 7. Comparison of the daily GCR dose rates measured simultaneously by the R3DE/R instruments in 2009

In Figure 3a, the lower end of the heavy arrows pointing “up” (along the Earth radius) in the R3DE photograph shows the exact place of the instrument. It is seen that it was surrounded by different constructive elements of the EuTEF platform and Columbus module, which produced additional shielding of the instrument against the SAA flux of 30-100 MeV protons. The R3DR position presented in Figure 3b shows that this instrument was far from the Zvezda module at the end of the EXPOSE-R facility and was practically shielded only from below.

The wide maximum observed on Figure 6b for L-values between 3.5 and 6.2 was connected with the registration of rare sporadic relativistic electrons precipitations (REP) generated in the outer radiation belt [25, 6-8]. Here the R3DR maximum of dose rate reached value of about $5000 \mu\text{Gy h}^{-1}$. This large dose is deposited by electrons with energies above 0.78 MeV. The R3DE ORB maximum was also lower and “thinner” than the R3DR maximum. The reason was same as the described above for the SAA maximum.

Figure 7 presents the result of comparison of the daily CGR dose rates for the period between 12 March and 20 June 2009 as measured by the R3DE/R instruments. The daily GCR dose rate was obtained by averaging of 5000-8200 measurements per day (7024 in average) with 10 s resolution at all latitudes in the altitudinal range 353-361 km above the Earth. Both data sets are situated in the bottom of the Figure and follow slowly decreasing with time trend, which can be associated with the decreasing altitude of the ISS from 360 down to 353 km. This trend is in opposite direction than the expected increase of the GCR dose rates with the increase of the Oulu Neutron monitor (NM) count rate shown with quadrats above the two dose rates curves. The Oulu NM count rate increase because of the decrease of solar activity in the end of the 23rd solar cycle. The decreasing solar activity leads to decrease of the amount and speed of solar wind and respectively decrease of the embedded magnetic field strength, which couldn't deflect effectively the GCR entering in the solar system.

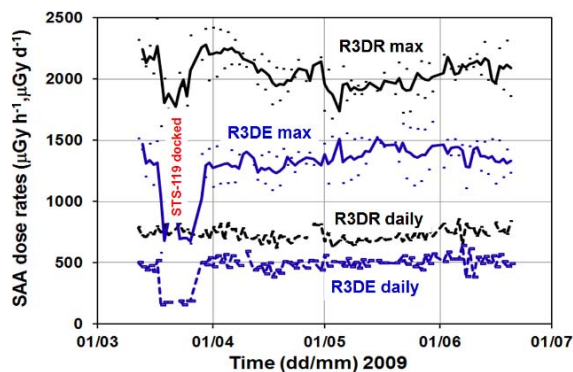


Fig. 8. Comparison of the daily SAA dose rates measured simultaneously by the R3DE/R instruments in 2009

The shapes of the dose rate curves are also strongly affected by the L value of the place where the averaged values was obtained. This is well seen when a comparison is made between the mean L curve in the top of the Figure 7 with the two daily dose rate curves in the bottom. L values are presented according to the right scale of the Figure. As expected there is almost positive correlation between them.

The difference between R3DE and R3DR dose rate data is about 10 $\mu\text{Gy d}^{-1}$ during the whole period of about 3 months. Relatively small part of this difference is produced by the additional dose rate produced by secondary particles in the heavily shielded R3DE instrument but another

mechanism have to be found to be described the difference. This will be subject of another more precise investigation with use of theoretical models.

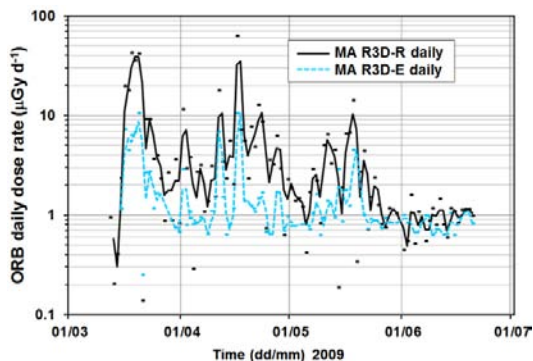


Fig. 9. Comparison of the daily ORB dose rates measured simultaneously by the R3DE/R instruments in 2009

In the bottom part of Figure 8 are shown the average daily dose rates obtained in the region of the SAA as measured by the R3DE/R instruments. The daily SAA dose rate was obtained by averaging of 400-500 measurements per day with 10 s resolution at all latitudes in the altitudinal range 357-361 km above the earth. In the top part of the figure the maximal observed per each day dose rates in $\mu\text{Gy h}^{-1}$ are presented. It is well seen that both curves of hourly and daily dose rates obtained by R3DR instrument are higher than the R3DE dose rates for the whole time interval between 12 March and 20 June 2009. The reason was already discussed in the presentation of Figure 6.

The strong depletion in the maximum dose rates in the left side of the Fig. 8 was generated by the additional shielding, which USA Space Shuttle 78 tons body on his mission STS-119 provided to both instruments when it was docked with the ISS (Dachev et al., 2011a).

Figure 9 shows moving averaged dose rates inside the ORB as measured by the R3DE/R instruments. The daily, average ORB dose rate over the whole period from R3DR is $4.9 \mu\text{Gy d}^{-1}$, while the daily, average ORB dose rate over the whole period from R3DE is about 3 times smaller - $1.7 \mu\text{Gy d}^{-1}$. The reason for the smaller dose rates measured by R3DE instrument is same as already described for the SAA dose rates.

Table 1. Comparison of the hourly and daily dose rates measured simultaneously by the R3DE/R instruments in 2009

SAA parameter	Average R3DR	Average R3DE	Comments
Hourly averaged absorbed dose rate (>500 meas. per day) ($\mu\text{Gy h}^{-1}$)	352	296	R3DR > R3DE
Daily averaged absorbed dose rate (in Si) ($\mu\text{Gy d}^{-1}$)	537	426	R3DR > R3DE
GCR parameter	Average R3DR	Average R3DE	Comments
Hourly averaged absorbed dose rate (>6000 meas. per day) ($\mu\text{Gy h}^{-1}$)	3.39	3.79	R3DE > R3DR
Daily averaged absorbed dose rate (in Si) ($\mu\text{Gy d}^{-1}$)	81.40	91.10	R3DE > R3DR
ORB parameter	Average R3DR	Average R3DE	Comments
Hourly averaged absorbed dose rate (no limit) ($\mu\text{Gy h}^{-1}$)	98.0	42.0	R3DR > R3DE
Daily averaged absorbed dose rate (in Si) ($\mu\text{Gy d}^{-1}$)	76.0	8.6	R3DR > R3DE

Table 1 summarizes the results of the observations made simultaneously by the R3DE/R instruments on ISS in 2009. The table practically presented by numbers the observations presented on Figures 6-10.

3.3. Empirical model for calculation of the absorbed dose rates in the extra vehicular environment of ISS at 359 km altitude

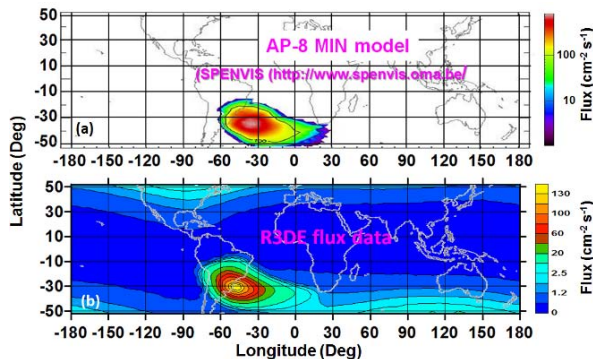


Fig. 10. Comparison of the global distribution of the R3DE flux data in the period 21 October 2008-24 February 2009 with the AP-8 MIN model

Figure 10 presents comparison of the global distribution of the R3DE flux data in the period 21 October 2008-24 February 2009 with the AP-8 MIN model. Figure 10b presented same data as shown in the Figure 5a. Figure 10a was created using the available in SPENVIS

(<http://www.spervis.oma.be/>) AP-8 MIN model [23] (Vette, 1991). The model is calculated for the epoch of 1970, for the minimum of the solar activity at altitude of 359 km and for protons with energy larger than 15.8 MeV. It is seen that the external oval of the data and the model are similar but the coordinates of the R3DE SAA was at -50° west longitude -30° south latitude. These values are in comparison with AP-8 MIN moved with -12° (0.3° per year) to the west and with 2° (0.05° per year) to the north and coincided relatively well with the values obtained by [16] Wilson et al., (2007). Another big difference between the model and the experimental data is seen for the value of the flux central location. The predicted by the model values were much higher than the observed. This can be explained by the fact that the R3DE SAA flux data are obtained in the end of the 2008 and beginning of 2009, which was in the period of extremely low solar activity not observed before and respectively not included in the AP-8 MIN model.

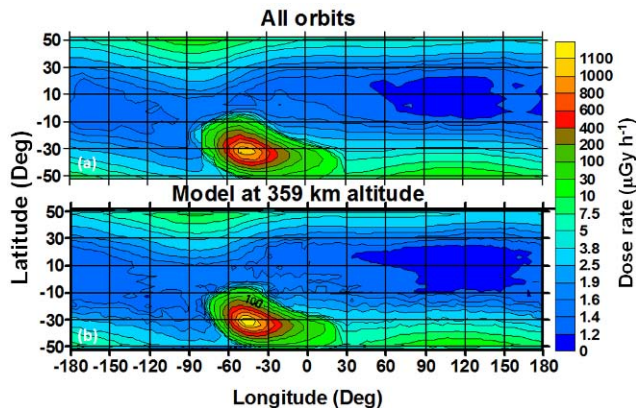


Fig. 11. Comparison of the global distribution of the R3DE dose rate data in the period 21 October 2008-24 February 2009 with the predicted by the empirical model data

The large data base obtained by the R3DE instrument was used for development of an empirical model for calculation of the absorbed dose rates from GCR and inner radiation belt protons in the extra vehicular environment of ISS at 359 km altitude. The model approximate the averaged in a grid empirical dose rate values to predict the values at required from the user geographical point, station orbit or area in geographic coordinate system [27]. The model is valid for the location of R3DE instrument outside the ISS at the EXPOSE-E platform behind 0.41 g cm^{-2} shielding. These predictions of the model could be used by space agencies

medical and other not specialized in the radiobiology support staff only for first rough approach in the ISS EVA time and space planning.

Figure 11 contains 2 panels. In the upper panel (Figure 11a) the global distribution of the R3DE averaged dose rates (in $\mu\text{Gy h}^{-1}$) data obtained in the period 21 October 2008-24 February 2009 was presented, while the lower panel (Figure 11b) presented the result of the calculated by the model global distribution of the dose rates. It is seen that both pictures are very similar and this verify that the model predicted well the dose rates in the areas of predominated inner belt energetic proton of the SAA region and areas of predominated GCR outside SAA in equatorial, middle and high latitudes.

The empirical model is available online from the following 2 links: http://www.stil.bas.bg/dwp/R3DE_POINT_model.zip and http://www.stil.bas.bg/dwp/R3DE_ORBIT_model.zip. Both links allowed

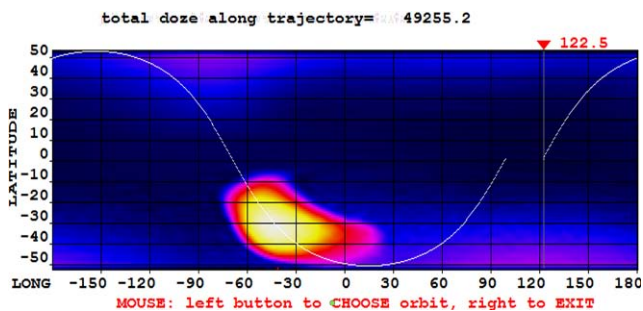


Fig. 12. Example of the graphical output from the “ORBIT” model for an orbit with ascending node equal to 122.5°

the possible user of the model to obtain for each model a compressed (ZIP) application (exe file), which directly in the computer of the user perform the calculation and present the result. The first link is for the so named “POINT” model, which calculated and presented the dose rate result (in $\mu\text{Gy h}^{-1}$) for a point with geographic coordinates inside of the set of coordinates with following limits: $-52^\circ < \text{Latitude} < 52^\circ$, $-180^\circ < \text{Longitude} < 180^\circ$. To calculate the dose it is necessary the obtained value to divide by 360.

The second link is for the so named “ORBIT” model, which calculated and presented the summarized dose rate results (in $\mu\text{Gy h}^{-1}$) along an orbit of the ISS, which ascending node is in the limit of -

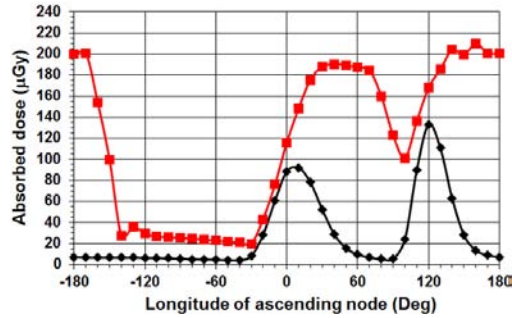


Fig. 13. Predicted by the model accumulated along the orbit absorbed dose for 1 orbit (~1.5 hours) (curve with diamonds) and 4 consecutive orbits (~6 hours) (curve with squares)

$180^{\circ} < \text{Longitude} < 180^{\circ}$. The step along the orbit is equal to 10 sec and is same as the R3DE time interval for 1 measurement.

Figure 12 presented one example of the graphical output from the “ORBIT” model for an ISS orbit with ascending node equal to 122.5° . The ascending node can be choosing by the user with movement of one arrow in the program and with pushing of the left mouse button. In the upper part after the label “total dose along trajectory” the calculated summarized dose rate is shown. To calculate the dose it is necessary the obtained value to divide by 360. Except the graphical output the model created automatically (in the directory where the model is) a text file with the following name “ORB_DOZ.TXT”. The file contains 4 columns: Lat. (deg), Long. (deg), Dose rate ($\mu\text{Gy h}^{-1}$) and the Accumulated till the moment dose rate ($\mu\text{Gy h}^{-1}$). If you use the model please reference Bankov et al. 2010, available online at <http://www.stil.bas.bg/FSR2009/pap144.pdf>

Figure 13 presents the predicted by the model accumulated along the orbit absorbed dose for 1 orbit (~1.5 hours) (curve with diamonds) and 4 consequent orbits (~6 hours) (curve with squares). The model was run with a longitudinal step of 10° for both cases. It is seen that for 1 orbit case the most dangerous ascending node is this crossing the equator at 120° East longitude when a total accumulated dose along the orbit of $139 \mu\text{Gy}$ is predicted. The 4 orbit case was chosen because usual EVA duration is about 6 hours, i.e. 4 orbits. The most dangerous ascending node for this case is this crossing the equator in the interval 140° East longitude to 170° West longitude when a total accumulated doses of about $200 \mu\text{Gy}$ are predicted.

3.4. Analysis of data collected by different instruments during real cosmonauts and astronauts EVA in the 2009-2010

3.4.1. Analysis of the dose rates and doses obtained during EVA2 of Expedition 18 on March 10, 2009. Example with predominant SAA crossings

Figure 14 purposes was: first to show the dose rate dynamics observed by R3DE and NASA TEPC

http://www.nasa.gov/mission_pages/station/research/experiments/TEPC.html

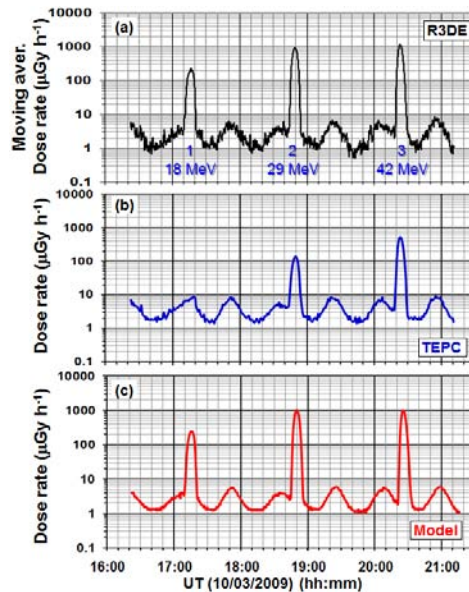


Fig. 14. The dose rate dynamics observed by R3DE and NASA TEPC during the EVA 2 of Expedition 18 on March 10, 2009 between 16:22 and 21:11 for 4 h and 49 m. Measured data was compared with the model predictions

during the EVA 2 of Expedition 18 on March 10, 2009 between 16:22 and 21:11 for 4 h and 49 m and second to compare the measured with R3DE instrument dose rates with the predicted by the model values.

Figure 15 supported the observations made on Figure 14 with actual information of the ground tracks of the ISS orbit during the EVA over the global maps of the R3DE measured dose rate and energy presented previously on Figure 5. The orbit numbers (1, 2 and 3) shown in Figure 14a correspond to the numbers on Figure 15a. Also the measured values of the

proton energy are shown, which according to Figure 15b increased from orbit number 1 to orbit number 3.

On Figure 14a the moving average (with period of 6 points (1 minute

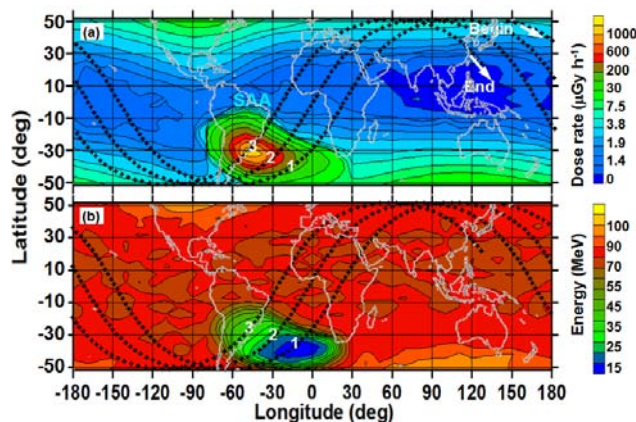


Fig. 15. Global maps of the R3DE measured dose rate and energy with the ground tracks of the ISS during the EVA shown on Figure 14. The numbers (1,2 and 3) in the region of the SAA corresponded to the number of SAA crossings seen on Figure 14

resolution)) of the dose rate measured by R3DE outside ISS behind less than 0.41 g cm^{-2} is presented. The labels on Figure 14a present the measured at the detector of the R3DE proton energy at the positions of the maximums, while Figure 15b presented the global map and it is identical to the Figure 5d. Very similar data with 1 minute resolution were plotted on Figure 14b, but from NASA TEPC situated inside ISS at physical location “SM-327”. Data were taken by [http://cdaweb.gsfc.nasa.gov/ server](http://cdaweb.gsfc.nasa.gov/server) [28]. Unfortunately we haven’t found what is the exact shielding of the TEPC at that location, but we consider that the shielding is much higher than the R3DE shielding. On Figure 14c were presented the calculated by the empirical model dose rates along the orbits of ISS. It is necessary to be mentioned that the 3 curves on Figure 14 coincided relatively very well by values and shape.

The 3 main maximums seen on figures 14a and 14b were created during the ISS crossings of the inner radiation belt high energy proton zone in the region of the SAA. R3DE dose rates maximums reached about $1000 \mu\text{Gy h}^{-1}$ for orbits 2 and 3 and only $250 \mu\text{Gy h}^{-1}$ for orbit number 1. The TEPC SAA maximums for orbits 2 and 3 are much smaller, while the SAA maximum for orbit 1 was completely missing. This feature can be explained by the R3DE measured proton energies shown on Figure 14a and on Figure 15b where the proton energy for orbit number 1 at the detector of

the R3DE was the smallest of all 3 and reach only 18 MeV. This proton energy wasn't enough for penetration of the larger shielding at the TEPC location inside ISS and that is why the maximum there is missing.

The maximums, which reached up to $9.5 \mu\text{Gy h}^{-1}$ in R3DE and TEPC data on Figure 14a and 14b are connected with the crossings at high latitude GCR regions in the both hemispheres, while the local minimums with dose rates around $1 \mu\text{Gy h}^{-1}$ and below correspond to the magnetic equator crossings. It is remarkable that the GCR TEPC dose rate data were always higher than the R3DE dose rates. Part of this higher exposition can be attributed to the additional dose rate created by secondary particles generated in the ISS walls. Another part is connected with the fact that TEPC having smaller sensitivity ($1 \mu\text{Gy h}^{-1}$) than R3DE overestimate the dose rates.

Table 2 presents the statistics for the total accumulated doses during the EVA2 of Expedition 18 on March 10, 2009 between 16:22 and 21:11 for 4 h and 49 m. Also the results of the separation of the doses accumulated by two different radiation sources – protons in the inner radiation belt, seen in the region of SAA, and GCR at low and high latitudes outside SAA are shown. The values for the R3DE and model doses were obtained using the

Table 2. Statistics of the measured and predicted doses in different locations during the EVA2 of Expedition 18 on March 10, 2009

Parameter	R3DE	TEPC	Model	Comments
Total accumulated absorbed dose (μGy)/equivalent dose (μSv) during the EVA	191/268	72/154	187	R3DE > TEPC
SAA accumulated absorbed dose (μGy)/equivalent dose (μSv) during the EVA	180/241	56/97	176	R3DE > TEPC
GCR accumulated absorbed dose (μGy)/equivalent dose (μSv) during the EVA	11/27	16/57	11	TEPC > R3DE

same periods along the orbit of ISS as the available information for the “Dominant radiation source at given time” in the <http://cdaweb.gsfc.nasa.gov/> server files. The R3DE ambient dose equivalent rates are calculated using the procedure described in [29].

The analysis of the Table 2 shows: 1) The SAA absorbed and equivalent doses predominate in the total doses for both instruments and the

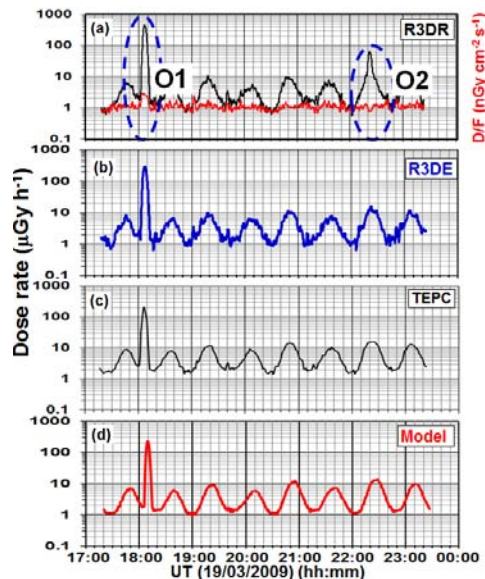


Fig. 16. The dose rate dynamics observed by R3DR, R3DE and NASA TEPC during the EVA 1 of STS-119 on March 19, 2009 between 17:16 and 23:23 for 6 h and 7 m. Measured data was compared with the model predictions

model; 2) The R3DE SAA absorbed doses were about 3 times higher than the TEPC doses because of the much smaller shielding of the R3DE detector; 3) The TEPC GCR absorbed and equivalent doses were higher than the R3DE doses. The possible reasons were discussed earlier; 4) There was a very good coincidence between the measured by the R3DE and predicted by the model doses.

3.4.2. Analysis of the dose rates and doses obtained during EVA 1 of STS-119 on March 19, 2009. Example with mixed SAA and outer radiation belt (ORB) relativistic electron precipitation (REP) crossings

Figures 16 and 17 form another pair of very similar content to the Figures 14 and 15. The 3D background of Figure 17 is identical to Figure 4 of Dachev et al., 2012b and presents the geographical distribution of the data for the period 01 April – 07 May 2010 when intensive REP was observed in the outer radiation belt region. The geographic longitude and latitude are on the X and Y axes, respectively. The white (white blue) curves represent equal McIlwain's L-parameter values [20, 21] (McIlwain, 1961;

Heynderickx et al., 1996) at the altitude of the ISS. The closed line in the eastern Hemisphere represents $L = 1$. Other open lines rise with values 1.5, 2.5, 3.5 and 4.5 from the equator toward the poles. The dose rate is in the 3rd dimension and the values are color coded by the logarithmic scale bar shown at the right side of the graphic. The dose rate values presented are obtained by averaging of the rough data in longitude/latitude squares 1° in size.

The REP regions were parts of the ORB and are seen in both hemispheres as bands of high dose rate values in the range $3.5 < L < 4.5$. The GCR dose rate values are also well seen in Fig. 17 as enhanced bands with values between 0.5 and $10 \mu\text{Gy h}^{-1}$ equatorwards from the REP bands.

The averaged L value distributions of the dose rates of the three major radiation sources are as follows: (1) GCR minimum average dose rate value is about $1 \mu\text{Gy h}^{-1}$ at $L = 1$. It rises up to $10\text{--}11 \mu\text{Gy h}^{-1}$ at $L = 4$ and stays at this value up to $L = 6.14$; (2) SAA dose rates are about $22 \mu\text{Gy h}^{-1}$ at $L = 1.1$. They rise sharply to a value of $600 \mu\text{Gy h}^{-1}$ at $L = 1.4$ and then slowly decrease to a value of $20 \mu\text{Gy h}^{-1}$ at $L = 2.8$; (3) ORB dose rates are at a value of $18 \mu\text{Gy h}^{-1}$ at $L = 3.15$, rise up to a value of $500 \mu\text{Gy h}^{-1}$ at $L = 4$ and then decrease down to a value of $80 \mu\text{Gy h}^{-1}$ at $L = 6.14$.

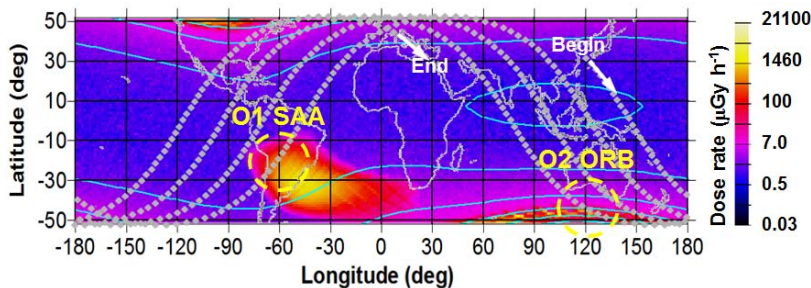


Fig. 17. Global maps of the R3DR measured dose rate with the ground tracks of the ISS during the EVA shown on Figure 16. The labels O1 and O2 corresponded to the number of SAA orbit crossings seen on Figure 16. The white (white blue) curves represent equal L -parameter values. South and north ORB regions are situated at $4.5 < L < 3.5$

Figure 16 is composed with similar dose rate dynamics observations as on Figure 14 but during the EVA 1 of STS-119 on March 19, 2009 between 17:16 and 23:23 for 6 h and 7 m. Here also is added the data obtained by the R3DR instrument. The maximum labeled with O1 is seen by all 3 instruments and by the model because it is formed during the crossings of the SAA South-West regions. Its dose rate is highest ($\sim 400 \mu\text{Gy h}^{-1}$) in

the R3DR data, which was less shielded than R3DR and TEPC instruments. The lowest dose rate is observed by the TEPC being inside ISS. The maximum labeled with O2 was seen only by the less shielded R3DR instrument. The maximum is formed inside of the South Hemisphere ORB region and the predominated radiation source in it was relativistic electrons with energies above 0.78 MeV. To prove this consideration on Figure 16a except the dose rate the dose to flux ratio is plotted. It is seen that the ratio in the O1 maximum is with values 2-3 nGy cm⁻² per particle, which is typical for protons with energies 30-50 MeV [30, 22] (Dachev, 2009; Heffner, 1971). The D/F values in the O2 maximum are less than 1 nGy cm⁻² per particle, which proved that predominant radiation source was from electrons [30, 22].

Table 3. Statistics of the measured and predicted doses in different locations during the EVA 1 of STS-119 on March 19, 2009 between 17:16 and 23:23 for 6 h and 7 m

Parameter	R3DR	R3DE	TEPC	Model
Total accumulated absorbed dose (μGy)/equivalent dose (μSv) during the EVA	57	45	47/142	37
SAA accumulated absorbed dose (μGy)/equivalent dose (μSv) during the EVA	32	23	16/28	14
GCR accumulated absorbed dose (μGy)/equivalent dose (μSv) during the EVA	18.6	22	31/114	23
ORB accumulated absorbed dose (μGy)/equivalent dose (μSv) during the EVA	5.2	0	0/0	0

Table 3 presented the statistics for the total accumulated doses during the EVA 1 of STS-119 on March 19, 2009 between 17:16 and 23:23 for 6 h and 7 m. Also the results of the separation of the doses accumulated by 2 different radiation sources – protons in the inner radiation belt, seen in the region of SAA and GCR at low and high latitudes outside SAA are shown. The values for the R3DE and model doses were obtained using the same periods along the orbit of ISS as the available information for the “Dominant radiation source at given time” in the <http://cdaweb.gsfc.nasa.gov/> server files.

The analysis of the Table 3 shows: 1) The GCR absorbed and equivalent doses predominate in the total doses for TEPC and the model; 2) The R3DR and R3DE SAA absorbed doses were higher than the TEPC

doses because of the much smaller shielding of their detectors; as expected there is a very good coincidence between the measured by the R3DE and the predicted by the model doses. The coincidence between the measured by the R3DR and predicted by the model doses is fair.

3.4.3. Analysis of the dose rates and doses obtained during EVA 1 of STS-131 on April 9, 2010. Example with predominant ORB REP crossings

The Space shuttle Discovery on the mission STS-131 docked with ISS at 07:44 UTC on 7th of April 2010 and undocked at 12:52 UTC on 17th of April 2010

http://www.nasa.gov/mission_pages/shuttle/shuttlemissions/sts131/launch/131_mission_overview.html. During the STS-131 mission on ISS 3 EVA were performed by the NASA astronauts Rick Mastracchio and Clayton Anderson on 9, 11 and 13 April 2010.

After the Coronal Mass Ejection (CME) at 09:54 UTC on 3 April 2010, a shock was observed at the ACE spacecraft at 0756 UTC on 5 April, which led to a sudden impulse on Earth at 08:26 UTC. Nevertheless, while

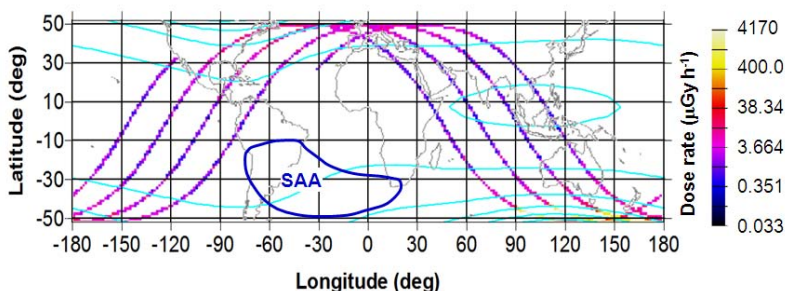


Fig. 18. Gray scale (color) coded dose rates along the trajectory of the ISS during the first EVA on 9th of April 2010. It is seen that the carefully chosen time of the EVA avoid SAA crossings. Highest dose rates are seen in the longitudinal range 90-150° in Southern Hemisphere

the magnetic substorms on 5 and 6 of April were moderate; the second largest in history of GOES fluence of electrons with energy >2 MeV was measured [7]. The R3DR data show a relatively small amount of relativistic electrons on 5 April. The maximum dose rate of 2323 $\mu\text{Gy day}^{-1}$ was reached on 7 April; by 9 April, a dose of 6600 μGy was accumulated. By

the end of the period on 7 May 2010 a total dose of 11,587 μGy was absorbed [7, 8].

Figure 18 presents the ISS trajectory during the EVA 1 on 9 April 2010 on the global map. As in Figure 17 the same L equal values lines are presented. The SAA place and surrounding curve are taken also from Figure 5 and shown here with a heavy line. The dose rate values along the trajectory of ISS are grey scale (color) coded by the logarithmic scale bar shown at the right side in Figure 18. It is seen that the ISS trajectories during the EVA were very carefully chosen by NASA radiologists to avoid crosses of the SAA high dose rates region. The GCR doses outside the relativistic electrons precipitation zones vary between $0.1 \mu\text{Gy h}^{-1}$ at the magnetic equator and $15 \mu\text{Gy h}^{-1}$ at high latitudes. Because of the outer radiation belt enhancement the astronauts were irradiated by the relativistic electrons. As seen they obtained the highest dose rates in the Southern Hemisphere at descending orbits at geographic latitudes above 42° South latitude. Precise analysis of the picture shows that when the trajectories

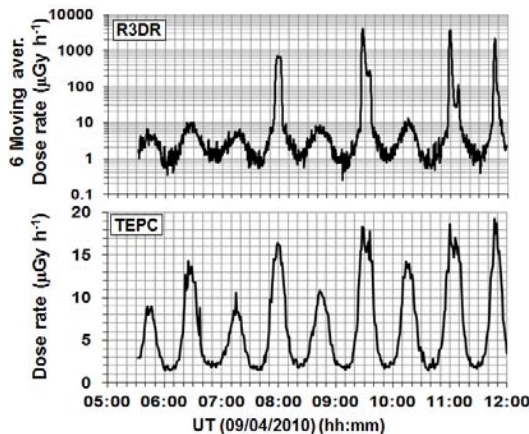


Fig. 19. The dose rate dynamics observed by R3DE and NASA TEPC during the EVA1 of STS-131 on April 9, 2010 between 05:31 and 11:58 UT for 6 h and 27 m

reached $L=3.5$ the color coded dose rates become white, i.e. they reach the maximum ($4170 \mu\text{Gy h}^{-1}$) of the code bar in the right hand side of Figure 18.

Figure 19 presents with usual 2D graphics the same dose rate dynamics as on Figure 18 observed by R3DE and NASA TEPC during the EVA 1 of STS-131 on April 9, 2010. The sinusoidal like meander of minimums and maximums shows the sequence of Northern and Southern Hemisphere crossings through the magnetic equator of the ISS high latitude

regions. Smaller maximums, excluding the last maximum, represented the Northern Hemisphere crossings, while the larger was observed in the Southern Hemisphere. The difference is because maximal L values in Northern Hemisphere are less than these in Southern Hemisphere. Looking precisely on the TEPC data it is possible to be seen that the energetic electrons outside ISS did enhance even the TEPC dose rates with few $\mu\text{Gy h}^{-1}$ and that the small maximums in TEPC data well coincide with much larger maximums in R3DR data. The TEPC dose rate maximums in REP regions can be associated even by direct impact of high energy electrons or with bremsstrahlung on the TEPC detector. Similar is the situation with the dose rate dynamics during other two EVAs on 11 and 13 April.

Figure 19 also presents how and where the TEPC overestimate the GCR dose rates. This is seen well in the minimal dose rates close to the magnetic equator. Here the minimal TEPC values are about $1 \mu\text{Gy h}^{-1}$, while at same places the more sensitive R3DR instrument measured much smaller dose rates reaching $0.25 \mu\text{Gy h}^{-1}$.

Keeping in mind that the average shielding of the space suit [1-3] (Anderson et al. 2003; Benton et al., 2006; Shurshakov et al. 2009) is very similar to the shielding of the R3DR detector we may conclude that a major

Table 4. Estimations of the doses obtained by American astronauts during 3 EVAs on 9th, 11th and 13th of April 2010.

Absorbed doses/Equivalent doses					
R3DR					TEPC (Zapp, 2011)
STS-131 EVA number	UTC from-to	GCR dose Gy/ Sv	ORB dose Gy/ Sv	Total Gy/ Sv	Total = GCR Gy/ Sv
EVA-1 6 h and 27 m	09/04/2010 05:31-11:58	17.6/49	443/443	461/492	41/138
EVA-2 7 h and 26 m	11/04/2010 05:30-12:56	18.6/53	269/269	288/322	49/163
EVA-3 6 h. and 24 m	13/04/2010 06:14-12:36	18.1/56	299/299	318/355	45/144
Total 20 h and 27 m		54.3/158.4	1012/1012	1067/1170	135/445

part of the astronaut's skins were irradiated with similar doses as the measured by R3DR instrument.

Table 4 summarizes the statistics for the 3 EVAs. It is seen that the GCR TEPC absorbed doses are more than 2 times larger than the R3DR doses. The measured by R3DR instrument ORB doses during the 3 EVAs was 443, 269 and 299 μGy respectively. In comparison with TEPC absorbed doses inside ISS the R3DR measured outside absorbed doses are 5-10 times larger for these 6-7 hours during EVAs. The difference for equivalent dose rates is about 2-3 times. (The R3DR ambient dose equivalent rates are calculated using the procedure described in (Spurny and Dachev, 2003).

The astronauts inside ISS collected during the docking with ISS between 7:44 hour on 7th of April and 12:52 at 17th of April 2010 totally 2766 μGy or 6663 μSv according to TEPC data. For the same period R3DR instrument behind 0.41 g cm^{-2} shielding collected much larger doses of 14523 μGy and 18187 μSv . If we will consider that the R3DR measurements during the three EVAs reflected the additional doses collected by the NASA astronauts outside ISS than we find in Table 4 that this is for 20 h and 27 m totally 1067 μGy or an enhancement of 38.6% in comparison to the astronauts being inside ISS. The equivalent additional dose according to R3DR data is 1170 μSv or an enhancement of 17.6%. Although the obtained doses do not pose extreme risks for the astronauts being on EVA they have to be considered as permanently observed source, which requires additional comprehensive investigations.

Conclusions

The paper analyzed the obtained results in the different radiation environments of Galactic Cosmic Rays, inner radiation belt trapped protons in the region of the South Atlantic Anomaly and outer radiation belt relativistic electrons during measurements with the Bulgarian build instruments on ISS. The obtained data was behind less than 0.41 g cm^{-2} shielding, which is very similar to cosmonauts and astronauts space suits shielding. These measurements results can be used by space agencies medical and other not specialized in the radiobiology support staff for first approach in the ISS extra vehicular activity time and space planning.

In conclusion, we would like to mention that the R3DE/R, low mass, dimension and price instruments, proved their ability to characterize the outside ISS radiation environment including the relativistic electron

precipitations. This was achieved mainly with the analysis of the deposited energy spectra, which was obtained at each measurement cycle of 10 s.

The main conclusion of the presented data is that REP events are common on the ISS. Although that the obtained doses do not pose extreme risks for astronauts being on EVA they have to be considered as a permanently observed source, which requires additional comprehensive investigations. An instrumental solution was proposed by Dachev et al., (2011b) where the possible hardware and software solutions for a new Liulin type dosimeter was proposed. New instrument will be able on the base of the analysis of the shape of the deposited energy spectrum and the value of the dose to flux ratio to distinguish the different kind of radiation sources in space as GCR, Inner radiation belt protons and outer radiation belt electrons and to calculate, store and present on display the absorbed and equivalent doses.

Acknowledgements

The authors are thankful to the following colleagues: G. Reitz, G. Horneck from DLR, Germany and D.-P. Häder, M. Lebert, M. Schuster from University of Erlangen, Germany for the cooperation in the development and operation of the R3DE/R instruments.

This work is partially supported by the Bulgarian Academy of Sciences and contract DID 02/8 with Bulgarian Science Fund.

References

- 1 . A n d e r s o n , B. M., et al. Analysis of a Radiation Model of the Shuttle Space Suit, NASA/TP-2003-212158, March 2003.
- 2 . B e n t o n , E.R., et al. (2006) Characterization of the radiation shielding properties of US and Russian EVA suits using passive detectors, Radiation Measurements, 41, 1191 – 1201, 2006.
- 3 . S h u r s h a k o v , V. A., et al. Solar particle events observed on MIR station, Radiat. Measur., 30, (3), 317-325, 1999.
- 4 . S i m p s o n J.A., in: Shapiro M.M. (Ed.) (1983) Composition and origin of cosmic rays, NATO ASI Series C: Mathematical and Physical Sciences. Vol. 107, Reidel, Dordrecht, 1983.
- 5 . K i m , M.-H.Y., et al. (2010) Probabilistic assessment of radiation risk for astronauts in space missions, Acta Astronautica, Volume 68, Issues 7-8, April-May 2011, Pages 747-759, 2010.

6. D a c h e v , Ts. P., et al. Relativistic Electrons High Doses at International Space Station and Foton M2/M3 Satellites, *Adv. Space Res.*, 1433-1440, 2009. doi:10.1016/j.asr.2009.09.023
7. D a c h e v , Ts., et al. Relativistic Electron Fluxes and Dose Rate Variations Observed on the International Space Station, published online in *JASTP*, 2012a. <http://dx.doi.org/10.1016/j.jastp.2012.07.007>
8. D a c h e v , Ts., et al. Relativistic Electron Fluxes and Dose Rate Variations during April-May 2010 Geomagnetic Disturbances in the R3DR Data on ISS, *Adv. Space Res.*, 50, 282-292, 2012b. <http://dx.doi.org/10.1016/j.asr.2012.03.028>
9. R e i t z , G., et al. Space radiation measurements on-board ISS—the DOSMAP experiment, *Radiat Prot Dosimetry*, 116, 374-379, 2005. <http://rpd.oxfordjournals.org/cgi/content/abstract/116/1-4/374>
10. B a d h w a r , G.D., et al. Radiation environment on the MIR orbital station during solar minimum. *Adv. Space. Res.* 22 (4), 501-510, 1998.
11. B e n t o n , E. R. a n d B e n t o n E. V. Space radiation dosimetry in low-Earth orbit and beyond, *Nucl. Instrum. And Methods in Physics Research, B*, 184, (1-2), 255-294, 2001.
12. NCRP. Radiation Protection Guidance for Activities in Low Earth Orbit. Report No. 142, Bethesda, MD, 2002.
13. D a c h e v , Ts., et al. Calibration Results Obtained With Liulin-4 Type Dosimeters, *Adv. Space Res.*, V 30, No 4, 917-925, 2002. doi:10.1016/S0273-1177(02)00411-8
14. D a c h e v , Ts., et al. Observations of the SAA radiation distribution by Liulin-E094 instrument on ISS, *Adv. Space Res.* 37 (9), 1672–1677, 2006.
15. N e a l y , J. E., et al. Pre-engineering spaceflight validation of environmental models and the 2005 HZETRN simulation code, *Adv. Space Res.*, 40, 11, 1593-1610, 2007. doi:10.1016/j.asr.2006.12.030
16. W i l s o n , J. W., et al. Time serial analysis of the induced LEO environment within the ISS 6A, *Adv. Space Res.*, 40, 11, 1562-1570, 2007. doi:10.1016/j.asr.2006.12.030
17. S l a b a , T.C., et al. Statistical Validation of HZETRN as a Function of Vertical Cutoff Rigidity using ISS Measurements, *Adv. Space Res.*, 47, 600-610, 2011. doi:10.1016/j.asr.2010.10.021
18. H o r n e c k , G., et al. Biological experiments on the EXPOSE facility of the International Space Station, *Proceedings of the 2nd European Symposium – Utilisation of the International Space Station*, ESTEC, Noordwijk, 16-18 November 1998, SP-433, pp. 459-468, 1998.
19. B e r g e r , M.J., et al. (2012) Stopping-Power and Range Tables for Electrons, Protons, and Helium Ions,. NIST Standard Reference Database 124, 2012. Available online at: <http://physics.nist.gov/PhysRefData/Star/Text/contents.html>
20. M c I l w a i n , C. E. (1961) Coordinates for mapping the distribution of magnetically trapped particles. *J. Geophys. Res.*, 66, pp. 3681-3691.
21. H e y n d e r i c k x , D., et al. Historical Review of the Different Procedures Used to Compute the L-Parameter. *Radiation Measurements*, 26, 325-331, 1996.
22. H e f f n e r , J., (1971) Nuclear radiation and safety in space, M, Atomizdat, pp. 115, 1971. (in Russian).

23. V e t t e , J. I. The NASA/National Space Science Data Center Trapped Radiation Environment Model Program (1964–1991). NSSDC/WDCR-R&S, 19–29, 1991.
24. H e y n d e r i c k x , D., et al. Calculating Low-Altitude Trapped Particle Fluxes With the NASA Models AP-8 and AE-8, Radiat. Meas., 26, 947-952, 1996.
25. W r e n n , G. L. (2009) Chronology of ‘killer’ electrons: Solar cycles 22 and 23, Journ. Atmos. Solar-Terr. Phys., 71, 1210-1218.
26. D a c h e v , T. P., et al. Space Shuttle drops down the SAA doses on ISS, Adv. Space Res., 47, 2030-2038, 2011a. doi:10.1016/j.asr.2011.01.034
27. B a n k o v , N. G., et al. Simulation model of the radiation dose measured onboard of the ISS, Fundamental Space Research, Supplement of Comptes Rend. Acad. Bulg. Sci., ISBN 987-954-322-409-8, 147-149, 2010. <http://www.stil.bas.bg/FSR2009/pap144.pdf>
28. Z a p , N. (2012) at NASA space Radiation Analysis Group, Johnson Space Center and by ‘Coordinated Data Analysis Web’ at Goddard Space Flight Center, (<http://cdaweb.gsfc.nasa.gov/>, June, 2012).
29. S p u r n y , F. a n d T s . D a c h e v . Long-Term Monitoring of the Onboard Aircraft Exposure Level With a Si-Diode Based Spectrometer, Adv. Space Res., 32, No.1, 53-58, 2003. doi:10.1016/S0273-1177(03)90370-X
30. D a c h e v , T s. P. Characterization of near Earth radiation environment by Liulin type instruments, Adv. Space Res., 44, pp 1441-1449, 2009. doi:10.1016/j.asr.2009.08.007
31. D a c h e v , T s. P. et al. Main Specifications of New Liulin Type Intelligent Crew Personal Dosimeter, Proceedings of Sixth Scientific Conference with International Participation SES, Sofia, 2-4 November 2010, ISSN 13131-3888, 76-82, 2011b. http://www.space.bas.bg/SENS/SES2010/1_SpPh/10.pdf
32. H ä d e r , D. P., et al. R3D-B2 - Measurement of ionizing and solar radiation in open space in the BIOPAN 5 facility outside the FOTON M2 satellite, Adv. Space Res. Volume 43, Issue 8, Pages 1200-1211, 2009. doi:10.1016/j.asr.2009.01.021
33. S t r e b , C., et al. R3D-B, Radiation Risk Radiometer-Dosimeter on Biopan (Foton) and expose on International Space Station, Proceedings of the Second Exo-Astrobiology workshop, Graz, Austria, ESA SP-518, 71-74, November 2002.

ОСОБЕНОСТИ НА КОСМИЧЕСКАТА РАДИАЦИЯ В ОБКРЪЖАВАЩОТО ПРОСТРАНСТВО НА МЕЖДУНАРОДНАТА КОСМИЧЕСКА СТАНЦИЯ (МКС)

Ц. Дачев, Н. Банков, Б. Томов, Ю. Матвийчук, П. Димитров

Резюме

Космическото време и свързаната с него йонизираща радиация се разглеждат като един от основните здравни проблеми на екипажа на Международната космическа станция (МКС). За да се определят радиационните ефекти върху хората е необходимо да се знае:

1) Натрупаната абсорбирана доза, която зависи от нейното глобално разпределение; 2) Локалното 3D разпределение на екраниращите маси. Радиометърът-дозиметърът на радиационния риск R3DE (Radiation Risks Radiometer-Dosimeter (R3D) за платформата EXPOSE-E на установката European Technological Exposure Facility (EuTEF) работи успешно извън европейския модул Columbus от м. февруари 2008 до м. септември 2009 г. Много подобен на него прибор, наречен R3DR, работи успешно в платформата EXPOSE-R извън руският модул „Звезда“ на МКС от м. март 2009 до м. август 2010 г. Двата миниатюрни спектрометри-дозиметри са от типа „Люлин“ и са разработени и изработени в България. Те натрупаха повече от 5 милиона измервания с 10 с. разрешение по време зад защита от 0.41 g cm^{-2} , която е много подобна на средната защита на американските и руските космически скафандри [1-3]. Това ни позволява да интерпретираме получените данни като възможни дози по време на работа на космонавтите извън стените на станцията Extra Vehicular Activities (EVA). В статията първо се анализират получените дългосрочни данни за: 1) Галактическата космическа радиация (GCR); 2) Захванатите във вътрешния радиационен пояс протони в района на южно-атлантическата аномалия (SAA) и 3) Релативистичните електрони във външния радиационен пояс (ORB). Голямата база от данни е използвана за създаването на емпиричен модел за пресмятане на абсорбираната доза в окръжаващата среда на МКС на височина от 359 км. Моделът апроксимира средната мощност на дозата в определена от потребителя: географска точка, орбита на станцията или площ в географска координатна система. В статията са показани сравнения на получените данни от приборите R3DE/R и приборът на NASA Tissue Equivalent Proportional Counter (TEPC) с модела по време на реални EVA на космонавти и астронавти в периода 2008-2010 г. Моделът е използван и за предсказване на акумулираните дози по дължината на орбитата на МКС за 1-ва орбита (1.5 часа) и за 4 последователни орбити (6 часа), което е обичайната продължителност на EVA. Тези предсказания могат да бъдат използвани от медицинския и другия неспециализиран в радиобиологията персонал на космическите агенции за определяне в първо приближение на възможната доза при планиране на времето и мястото на бъдещи EVA.